Journal of Biomolecular NMR, 3 (1993) 639–652
ESCOM

J-Bio NMR 154

$^{13}C^{\alpha}$-NMR assignments of melittin in methanol and chemical shift correlations with secondary structure

Paul Buckley[a], Arthur S. Edison[b], Marvin D. Kemple[c] and Franklyn G. Prendergast[a,*]

[a]*Department of Biochemistry and Molecular Biology, Mayo Foundation, Rochester, MN 55905, U.S.A.*
[b]*Biophysics Program, University of Wisconsin, Madison, WI 53706, U.S.A.*
[c]*Department of Physics, IUPUI, Indianapolis, IN 46202-3273, U.S.A.*

Received 20 May 1993
Accepted 22 August 1993

Keywords: NMR; Peptide; CD; Alpha-helix; Melittin

SUMMARY

Melittin is a naturally occurring hexacosa peptide which forms an amphiphilic helix in methanol, a random coil in water, and a tetramer of helices at basic pH or in the presence of a high salt concentration. The monomeric structure in methanol has been well characterized by proton NMR (Pastore et al. (1989) *Eur. Biophys. J.*, **16**, 363–367). In the present paper, chemical shifts of the backbone α-carbons of melittin in methanol were determined by mapping previously published α-proton shifts (Bazzo et al. (1988) *Eur. J. Biochem.*, **173**, 139–146), to natural abundance $\{^1H\}^{13}C$ cross peaks appearing in the 2D heteronuclear multiple-quantum NMR spectrum. Changes in chemical shifts consequent to stepwise increases in the percentage of water in a mixed methanol/water solvent system were observed in similar spectra. The α-carbon shifts varied more smoothly than the corresponding α-proton shifts and were found to correlate with the transition from the helix to the random coil conformer in parallel with changes in the circular dichroism spectrum. Chemical shifts of this peptide are interpreted with regard to the current database of assignments in proteins of known 3D structure (Wishart et al. (1991) *J. Mol. Biol.*, **222**, 311–333). The N-terminal region of the peptide shows increased flexibility at lower methanol concentrations, as evidenced by the merger of the α-proton resonances of G1 (at 40% and 15% methanol) and G3 (at 15% methanol). Conformational exchange rates for G1 and G3 were estimated by comparison of the experimental spectra with simulated spectra and found to be as large as 4000 s^{-1} for G1 in 40% and 15% methanol and 600 s^{-1} for G3 in 15% methanol. Overall, these ^1H and ^{13}C chemical shift data support the description of monomeric melittin in methanol currently evolving in the literature and suggest a structure composed of a linked pair of helices with different structural stabilities, each of which experiences dynamical fraying at its free terminus.

INTRODUCTION

Melittin is a well-characterized 26-amino acid peptide from the venom of the *Apis mellifera* honey bee (Bello et al., 1982; Quay and Condie, 1983; Dempsey, 1988; Pastore et al., 1989;

*To whom correspondence should be addressed.

Weaver et al., 1989; Lakowicz et al., 1990). The sequence is H_2N-GIGAV$_5$-LKVLT$_{10}$-TGLPA$_{15}$-LISWI$_{20}$-KRKRQQ-NH_2 (Habermann, 1972). High-resolution NMR has been used to describe three conformational states which can be established in solution by varying solvent conditions – a random coil monomer, a nearly symmetric protein-like aggregate of four helices, and a monomeric amphipathic helix (Brown et al., 1980; Lauterwein et al., 1980; Bazzo, 1988). Bazzo et al. have determined the proton chemical shift assignments of the monomeric helix in perdeuterated methanol by 2D NMR and modeled the structure by using molecular dynamics with NOE-derived distance constraints. The crystal structure of the tetrameric aggregate has been solved to 2 Å resolution (Terwilliger and Eisenberg, 1982 a,b) and has been correlated with the monomeric α-helical structure described by molecular dynamics (Pastore et al., 1989). Melittin has also proven to be a useful model for controlled studies of protein folding as well as for peptide-lipid interactions (Ikura et al., 1991; Weaver et al., 1992; Wilcox and Eisenberg, 1992).

The interpretation of heteronuclear chemical shifts in terms of secondary structure is increasingly being used as heteronuclear NMR techniques continue to develop. As an example, the chemical shifts of nitrogen nuclei were recently shown to be sensitive to hydrogen bond length and secondary structure (Zhou et al., 1992). Also, Wishart et al. (1991) have summarized the conformational dependencies of α-carbon chemical shifts in a group of six proteins of known structure and noted that the wider frequency dispersion of α-carbon nuclei may allow them to be used as a more sensitive measure of main-chain conformation than either proton shifts or coupling constants. Using an overlapping set of four well-characterized proteins, Spera and Bax (1991) have reported correlations between both $^{13}C^{\alpha}$ and $^{13}C^{\beta}$ chemical shifts and the associated ϕ and ψ angles in crystal structures. They demonstrated that the distribution of deviances of α-carbon chemical shifts from random coil values, averaged over all residue types, is well separated between α-helix and β-sheet regions. In the similar database examined by Wishart et al. (1991), $^{13}C^{\alpha}$ shifts from different amino acid types are not averaged but are tabulated individually, and some amino acids appear in non-overlapping chemical shift ranges corresponding to different secondary structures; among them arginine and glutamine are most notable for having large separations in chemical shifts between helical and extended forms.

We have correlated assignments for the α-protons, and some β-protons, of melittin in methanol with their associated carbon chemical shifts using heteronuclear 2D NMR. Region-specific details of the helix stability were observed by monitoring the change in chemical shift of the α-carbons along the transition from the monomer helix in methanol to the monomer random coil in water. Chemical shift results are reported relative to the values found for the maximally helical form and are also related to the β-strand and α-helix values tabulated thus far for proteins. The description of secondary structure derived from the NMR results is discussed with respect to the ellipticity of the melittin CD spectrum.

MATERIALS AND METHODS

Melittin was prepared with an amidated C-terminus by solid-phase synthesis using t-BOC

Abbreviations: NMR: nuclear magnetic resonance, CD: circular dichroism, NOE: nuclear Overhauser enhancement, NMRFAM: Nuclear Magnetic Resonance Facility at Madison, HMQC: Heteronuclear Multiple Quantum Correlation, COSY: Correlated Spectroscopy, TOCSY: Total Correlated Spectroscopy, $[\theta]_{xxx}$: molar ellipticity at xxx nm, TFE: trifluoroethanol, δ (ppm): chemical shift in parts per million, Δδ: secondary chemical shift (difference from random coil shift).

chemistries and methylbenzhydrilamine resin on an Applied Biosystems model 430 Peptide Synthesizer. Derivatized amino acids were purchased from Applied Biosystems. Cleavage products were separated by reverse-phase high-pressure liquid chromatography, using a ramp of 0% to 80% acetonitrile in 0.1% trifluoroacetic acid. Purity was determined by fast atom bombardment mass spectrometry, amino acid composition analysis, and N-terminal peptide sequencing.

For natural abundance NMR studies, melittin was dialyzed against H_2O, titrated in D_2O with dilute DCl and NaOD to approximately pD 5, and lyophilized three times from D_2O. Peptide samples at 7 mM were prepared in CD_3OD/D_2O cosolvents at 100, 90, 80, 70, 60, 40 and 15 w/w% CD_3OD (corresponding to 100.0, 83.5, 69.2, 56.8, 45.8, 27.3, and 9.0 mol/mol%). Concentrations of all samples were verified by the single Trp absorbance at 280 nm, $\varepsilon = 5600\ M^{-1}\ cm^{-1}$.

HMQC experiments (Müller, 1979; Bax et al., 1983) were collected on Bruker AM-500 spectrometers at 25 °C in the reverse detection mode at the NMRFAM. 2048 or 4096 data points with a 145-μs dwell time and 512 experiments with a 66- or 62-μs dwell time were collected in t_2 and t_1, respectively. The carrier frequencies were 500.139 MHz (t_2) and 125.635 MHz (t_1), and the period to generate antiphase coherence ($1/2J_{CH}$) was set to 3.57 ms. WALTZ decoupling was used during acquisition to decouple protons from their attached ^{13}C carbons and a DANTE pulse sequence was employed in some samples to suppress the residual water signal. Residual protonated methanol (CHD_2OD) was used as an internal reference, uncorrected for dilution (see below), with chemical shift values of 48.90 ppm for carbon and 3.30 ppm for proton. Methanol chemical shifts were determined using external central capillary reference standards: neat dioxane at 67.37 ppm for carbon and TSP in D_2O at 0.0 ppm for proton. A TOCSY experiment (Braunschweiler and Ernst, 1983) was performed on the 100% CD_3OD sample to aid in the spectral assignment process with 4096 data points and 256 experiments with a dwell time of 98 μs and a mixing time of 50.54 ms. Two-dimensional data sets were processed and analyzed by using Felix software (Hare Research, Inc., Woodinville, WA, U.S.A.) with and without exponential filters in t_2 and 90° phase-shifted-squared sinebell functions in t_1, and zero-filled to 4096 real points in both dimensions.

Circular dichroism spectra were collected on a computer controlled Jasco J-500A spectropolarimeter standardized with *d*-camphor-10-sulfonic acid. Measurements were made at 20.0 °C with 0.1-cm path length cuvettes on 30-μM melittin samples. Solvent mixtures corresponding to 97.00, 86.47, 74.93, 51.40, 41.45, 20.81 and 7.64 w/w% CD_3OD/D_2O (95.28, 79.98, 65.13, 39.79, 31.68, 14.10, and 4.93 mol/mol%) were prepared from an unbuffered aqueous stock solution of 0.255-μM melittin and deuterated methyl alcohol. Data were collected in a single scan and smoothed with a five-point running average after baseline subtraction. Deuterated reagents were purchased from Cambridge Isotope Laboratories and Wilmad Glass Co.

RESULTS

CD spectra of melittin in the various cosolvent mixtures are shown in Fig. 1. The appearance of a single isodichroic point, for all but the two spectra of samples with the lowest proportion of methanol, indicates a simple transition from helix to random coil form with decreasing methanol concentration in the solvent system. In 100% CD_3OD, melittin has a $[\theta]_{222}$ of -26 deg cm^2 dmol^{-1}, by extrapolation from the collected data, which corresponds to a maximum of 65% helicity (or 17 residues) based on the value of -40 deg cm^2 dmol^{-1} for maximum helicity in designed peptides at

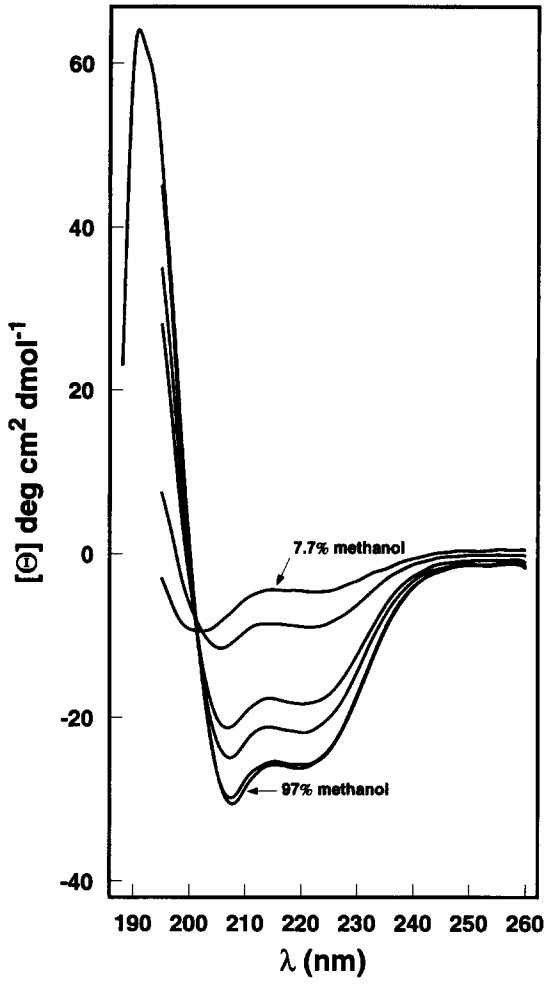

Fig. 1. Circular dichroism spectra of 30-μM melittin in CD_3OD/D_2O solvent mixtures at 20.0 °C. Weight percent CD_3OD: 7.64, 20.81, 41.45, 51.40, 74.93, 86.47, and 97.00. Single acquisitions were smoothed with a five-point running average after subtraction of solvent blanks of methanol and water in relative volume proportions.

20.0 °C determined by Merutka et al. (1991). Equation 1 of Greenfield and Fasman (1969) assumes an extremum at 208 nm of −33 deg cm^2 $dmol^{-1}$ with a correction for the contribution from β-sheet and random coil forms:

$$\% \ \alpha \text{ helix} = \frac{[\theta]_{208} - 4}{30 - 4}$$

Calculation by this method, which is based on the $[\theta]_{208}$ of poly-L-lysine at 22 °C, gives a maximum helicity of 92% at 97% CD_3OD (−30.6 deg cm^2 $dmol^{-1}$) and approaches 97% helix by extrapolation to 100% CD_3OD. ^1H and ^{13}C resonance assignments in the HMQC spectra, given in Tables 1 and 2, were based on the proton chemical shifts determined by Bazzo et al. (1988) and standard carbon chemical shifts (Wishart et al., 1991). $\{^1H\}^{13}C^{\alpha}$ and $\{^1H\}^{13}C^{\beta}$ peaks in the 100%

TABLE 1
PROTON CHEMICAL SHIFT ASSIGNMENTS[a] OF MELITTIN IN METHANOL/WATER MIXTURES

Residue[b]	100[c]	90[c]	80[c]	70[c]	60[c]	40[c]	15[c]
G1	3.94	3.96	3.95	3.90	3.95	3.87	3.87
G1	3.85	3.84	3.85	3.85	3.88	3.87	3.87
I2	4.03	4.06	4.10	4.13	4.14	4.18	
G3	3.74	3.75	3.77	3.78	3.79	3.83	3.89
G3	3.88	3.91	3.91	3.89	3.92	3.91	3.89
A4	4.07	4.09	4.12	4.15	4.17	4.22	4.28
V5	3.58	3.60	3.65	3.70	3.74	3.75	3.83
L6	4.06	4.07	4.10	4.11	4.12	4.18	4.23
K7	4.06	4.07	4.08	4.10	4.11	4.16	4.25
V8	3.69	3.72	3.76	3.81	3.84	3.92	
L9	4.13	4.15	4.17	4.20	4.22	4.29	4.36
T10	4.15	4.19	4.21	4.24	4.26	4.29	4.20
T11	4.31	4.32	4.33	4.34	4.34	4.34	
G12	4.10	4.11	4.12	4.11	4.09	4.07	4.03
G12	3.94	3.97	3.98	3.99	4.00	4.00	3.96
L13	4.39	4.39	4.40	4.40	4.41	4.42	4.47
P14	4.23	4.22	4.22	4.21	4.21	4.23	4.32
P14δ	3.77	3.78	3.79	3.79	3.79	3.82	3.72
A15	4.14	4.15	4.15	4.15	4.16	4.17	4.20
L16	4.23	4.23	4.24	4.23	4.24	4.25	4.27
I17	3.73	3.72	3.73	3.73	3.73	3.85	
S18	4.10	4.11	4.13	4.03	4.14	4.15	4.06
S18β	4.10	4.10	4.10	4.09	4.06	4.03	3.85
S18β	3.98	4.00	4.00	3.99	3.99	3.97	3.81
W19	4.30	4.29	4.30	4.30	4.29	4.31	4.38
I20	3.50	3.47	3.46	3.45	3.45	3.45	3.56
K21	3.88	3.89	3.89	3.88	3.91	3.92	4.00
R22	4.04	4.03	4.03	4.03	4.04	4.05	4.11
K23	3.94	3.91	3.91	3.90	3.90	3.92	4.00
R24	4.05	4.06	4.08	4.08	4.09	4.11	4.16
Q25	4.11	4.13	4.14	4.15	4.16	4.18	4.24
Q26	4.18	4.19	4.20	4.18	4.19	4.22	4.25

[a] Referenced to internal CHD_2OD at 3.30 ppm.
[b] Chemical shifts are for α-protons unless otherwise noted. Glycine geminal protons are listed separately.
[c] Percent (%) by weight of CD_3OD in deuterated methanol/water mixtures.

CD_3OD spectrum were mapped directly from the Bazzo et al. proton assignments to our spectra within 0.01 ppm with few exceptions. The correlation between the previously published and current α-and β-proton chemical shifts in 100% deuterated methanol are shown in Fig. 2. It is clear from the 100% CD_3OD HMQC spectrum, sections of which are shown in Fig. 3, that the S18 α-proton and one of its β-protons have the same chemical shift and that the two β-protons are distinct in the proton dimension. These assignments for S18 do not agree with the values determined from proton spectra alone (Bazzo et al.). The Q26 α-proton is shifted upfield in our study relative to the original work (4.17 ppm vs. 4.36 ppm) and the Q25 α-proton is shifted slightly

downfield (4.11 ppm vs. 4.09 ppm). We do not have an explanation for this but in both cases the HMQC assignments agree with the two AM(PT)X spin systems found in the 100% methanol TOCSY spectrum (not shown). Although the G1 and G3 α-proton chemical shifts differ from the values reported by Bazzo et al. by as much as 0.10 ppm (see Fig. 2), the terminal glycines are clearly identifiable in the HMQC. Assignments in the spectra from CD_3OD/D_2O solvent mixtures were made by comparison with the next less dilute sample spectrum, i.e., the 90% CD_3OD spectrum was assigned from the 100% CD_3OD spectrum, and so forth. The changes between spectra were small enough to allow this comparative assignment procedure to proceed unambiguously. However, some peaks were not observed in the spectrum of melittin in 15% CD_3OD.

While both the carbon and proton chemical shifts of the residual CHD_2OD were expected to change due to dilution with D_2O, variations in their values between spectra were assumed to be

TABLE 2
CARBON CHEMICAL SHIFT ASSIGNMENTS[a] OF MELITTIN IN METHANOL/WATER MIXTURES

Residue[b]	100[c]	90[c]	80[c]	70[c]	60[c]	40[c]	15[c]
G1	42.27	42.40	42.21	42.15	41.97	41.98	41.84
I2	62.16	61.92	61.70	61.44	61.23	60.84	
G3	46.22	46.09	45.86	45.56	45.39	44.84	44.22
A4	54.40	54.28	53.95	53.58	53.27	52.55	51.70
V5	65.67	65.42	65.01	64.50	64.12	63.34	62.48
L6	57.23	57.06	56.78	56.42	56.08	55.72	55.25
K7	58.93	58.73	58.38	57.97	57.67	56.79	55.79
V8	66.10	65.75	65.27	64.71	64.23	63.10	61.79
L9	56.69	56.77	56.43	56.17	55.87	55.22	54.43
T10	64.32	63.85	63.42	62.98	62.53	61.88	60.47
T11	63.46	63.12	62.83	62.51	62.19	61.69	59.72
G12	45.01	44.84	44.69	44.44	44.27	44.03	43.79
L13	58.46	58.16	57.95	57.61	57.16	56.51	54.94
P14	65.83	65.81	65.73	65.62	65.42	63.04	61.14
P14δ	49.14	49.15	49.12	49.08	49.05	49.01	
A15	54.41	54.31	54.16	53.97	53.77	53.51	52.79
L16	57.60	57.42	57.39	57.22	57.03	56.78	55.90
I17	64.15	64.08	63.98	63.86	63.67	63.07	61.77
S18	61.90	61.67	61.55	61.30	61.20	60.77	58.59
S18β	62.24	62.15	62.15	62.06	61.96	61.79	60.95
W19	60.70	60.69	60.57	60.58	60.30	60.00	59.13
I20	64.89	64.77	64.65	64.55	64.32	63.81	63.05
K21	59.60	59.48	59.31	59.18	58.85	58.50	57.43
R22	58.21	58.19	58.03	57.94	57.70	57.36	56.52
K23	57.44	57.30	57.17	57.06	56.83	56.60	56.01
R24	57.58	57.44	57.17	57.01	56.78	56.44	55.85
Q25	56.71	56.54	56.34	56.21	56.01	55.38	54.65
Q26	55.53	55.42	55.26	55.13	55.03	54.88	54.56

[a] Referenced to internal CHD_2OD at 48.90 ppm.
[b] Chemical shifts are for α-carbons unless otherwise noted.
[c] Percent (%) by weight of CD_3OD in deuterated methanol/water mixtures.

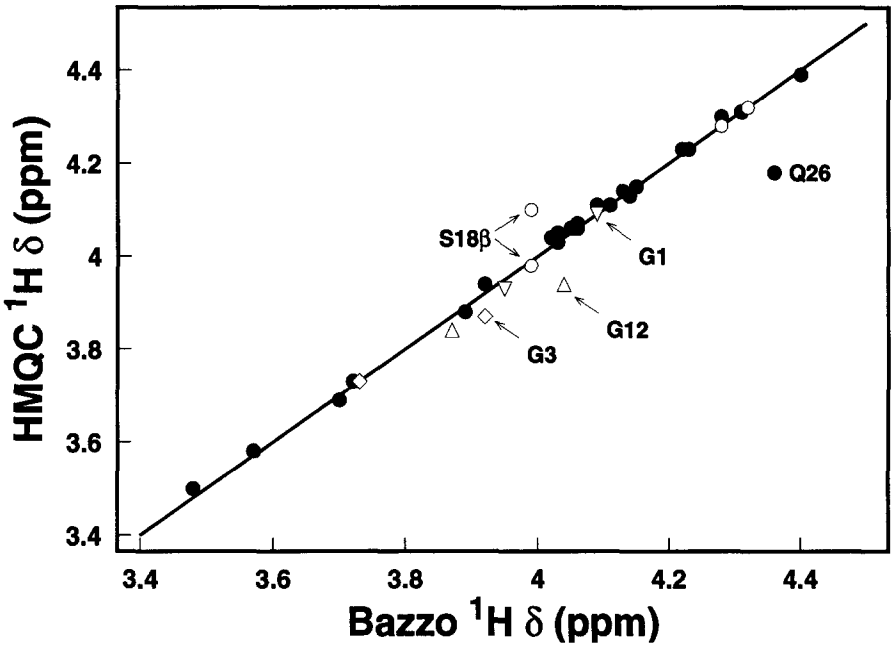

Fig. 2. Comparison between proton chemical shift assignments used here and published values (Bazzo et al., 1980) for melittin 100% in CD_3OD. The line is drawn for reference to a perfect correlation. Data points are (●) for α-protons and (○) for β-protons. The geminal proton pairs are shown for G1(▽), G3(◇), G12(△), and S18β(○).

small compared with changes typically observed for the melittin α-resonances (Tables 1 and 2) and not appreciably larger than the experimental errors. This assumption was corroborated by the behavior of the P14 δ signals which provided a non-backbone reference to chemical shift changes due to solvent composition. The P14 δ-carbon resonance shifted less than 0.04 ppm between individual steps of the CD_3OD concentrations examined and only 0.13 ppm over the entire range, although a trend toward a lower carbon chemical shift was observable over the range studied. In addition, observations of the methanol chemical shift in a separate series of 100% to 15% methanol/water mixtures, independently referenced to an external standard in a concentric capillary, indicate a chemical shift change of less than 0.02 ppm for the proton and less than 0.13 ppm for the carbon resonances. Consequently, the ^{13}C data shown are not corrected for deviations from the reference peak assignment of 48.90 ppm. Similarly, the P14 δ-proton resonance shifts less than 0.02 ppm over the course of the titration which, while on the order of some of the other proton chemical shift changes, is an order of magnitude less than the largest changes observed. The ^1H reference assignment was not corrected for deviations from 3.30 ppm.

Figure 4 depicts the changes in chemical shifts in both the proton and carbon dimensions with dilution of the CD_3OD with D_2O. The differences have been calculated to place most of the numbers on a positive scale; the carbon resonances migrate upfield as the peptide is observed in stages of uncoiling from 100% CD_3OD toward 100% D_2O while the proton resonances shift downfield. Exchange between peptide helix and random coil environments is fast on the NMR time scale (Schwarz, 1965) so that a single peak with an averaged chemical shift is observed for a given carbon or proton in exchanging residues.

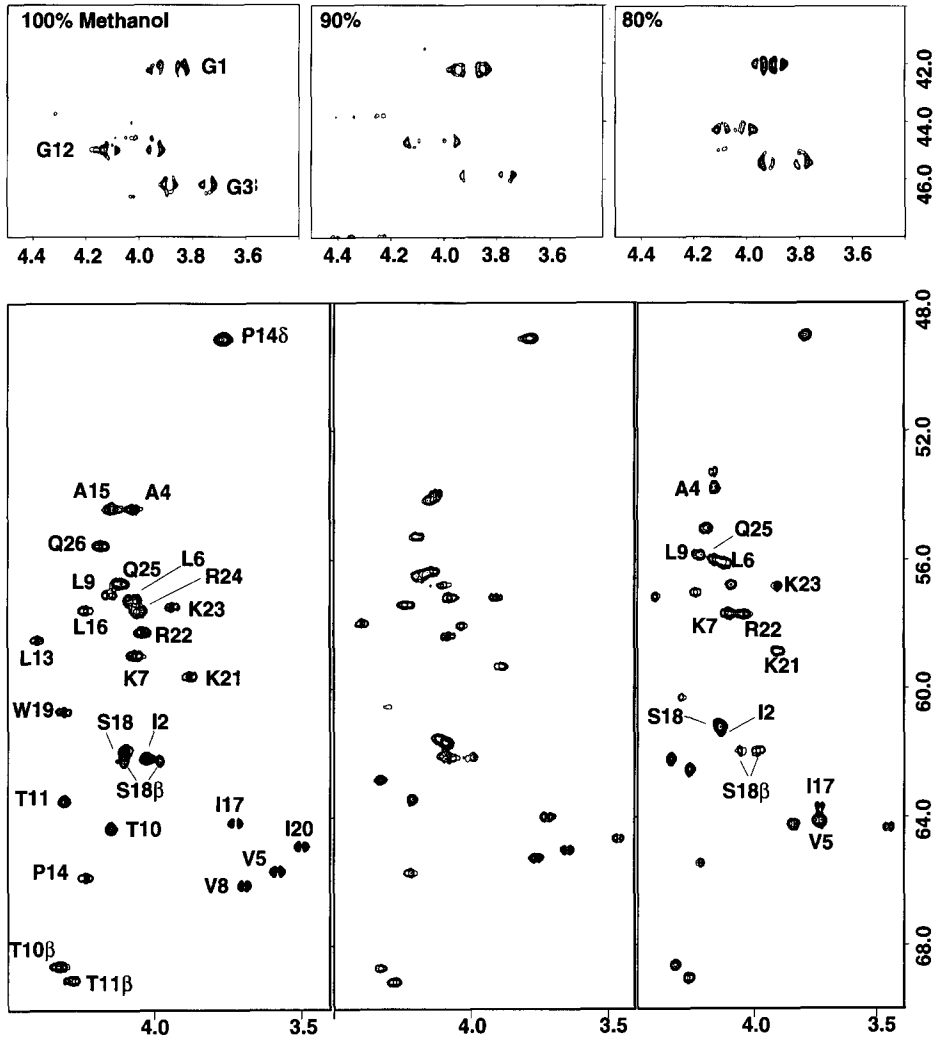

Fig. 3. Regions of the 500-MHz HMQC spectra of natural abundance melittin in 100%, 90%, and 80% CD_3OD/D_2O showing the α-, some β-, and P14δ proton-carbon cross peaks. Chemical shifts are referenced to residual protonated methanol uncorrected for solvent composition. The small splittings in the proton dimension are due to proton–proton scalar coupling; directly attached ^{13}C resonances are decoupled.

As can be seen from Fig. 3, the two α-proton signals from each of G1, G3, and G12 are resolved to different degrees in a solvent dependent manner. The separation of the α-proton signals for each of the three glycines generally decreases as the solvent is changed from 100% to 15% CD_3OD. In particular, the α-proton signals from G1 merge into one signal at both 40% and 15% CD_3OD, those from G3 merge at 15% CD_3OD, and those from G12 remain distinct at all methanol concentrations studied. These results are also consistent with the observations made by Lauterwein et al. (1980) for monomeric (random coil) melittin in 100% D_2O in which the uniqueness of one set of glycine geminal protons was used to make the G12 assignment.

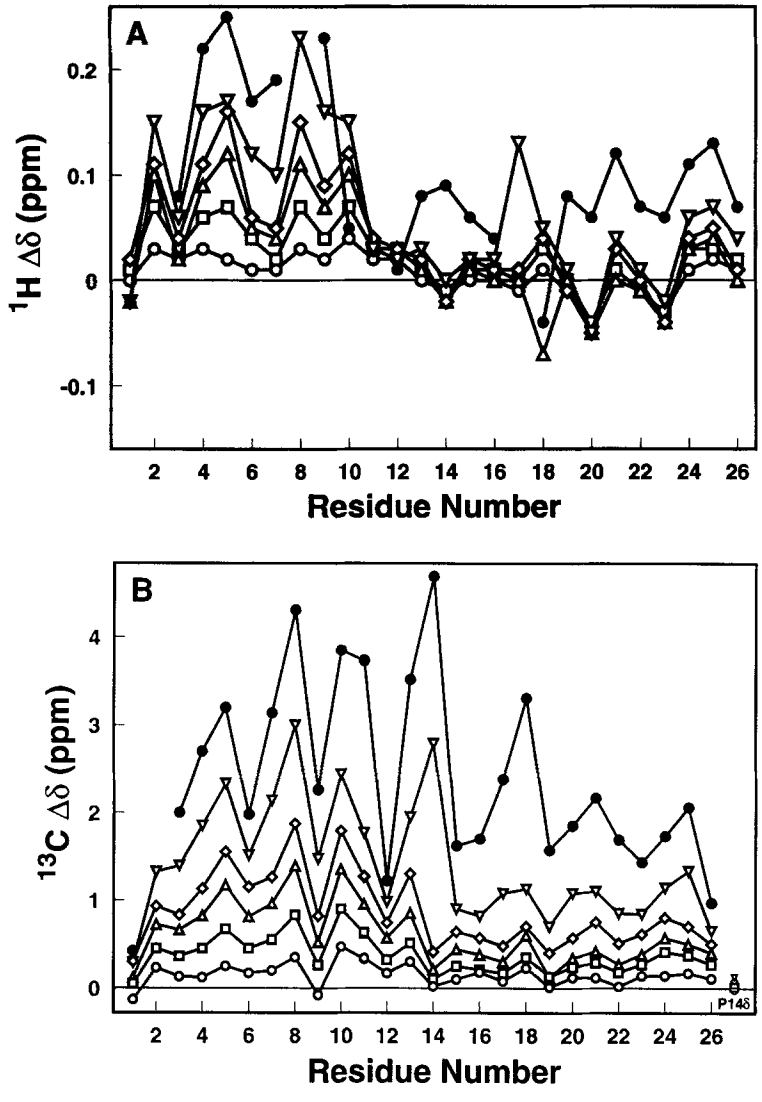

Fig. 4. (A) The difference in chemical shift of the melittin α-protons in the various CD_3OD/D_2O solvent mixtures from the 100% CD_3OD assignments ($\Delta\delta = \delta(^1H)_x - \delta(^1H)_{100}$). (B) The difference in chemical shift of the melittin α-carbons in the 100% CD_3OD from the CD_3OD/D_2O solvent mixture assignments ($\Delta\delta = \delta(^{13}C)_{100} - \delta(^{13}C)_x$). The change in chemical shift with solvent of the ^{13}C-P14δ resonance is shown in (B) for comparison. Samples were 7 mM in weight percent CD_3OD; (○) 90%, (□) 80%, (△) 70%, (◇) 60%, (▽) 40%, and (●) 15%.

DISCUSSION

Melittin provides a convenient and interesting model for directly probing the characteristics of peptide chain differences between the random coil, α-helix, and protein-like conformations. The site-specific and conformation-dependent chemical shift changes over the whole of the melittin molecule provide an insight into a diverse structural system within the 26 amino acids of the polymer. These observations with melittin establish the model as a basis for exploration of

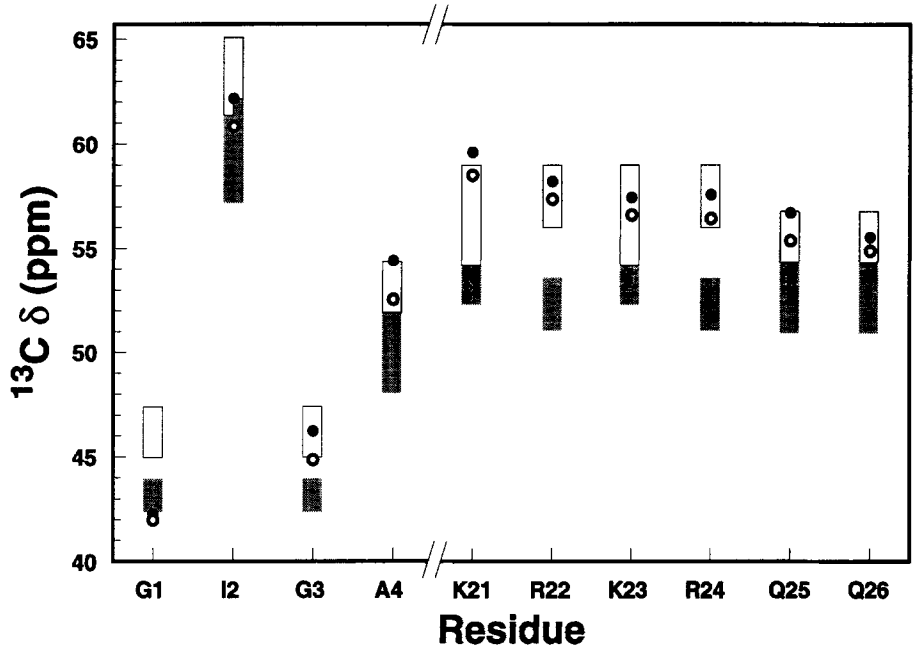

Fig. 5. Chemical shifts of some of the melittin α-carbons in 100% and 40% CD_3OD (filled and open circles, respectively) and the range of α-carbon chemical shift values (bars) which encompasses about 90% of the values found in proteins as reported in Fig. 4 of Wishart et al. (1991). Filled bars represent the distribution in β-strands and open bars represent that of α-helices. The noted ranges overlap for isoleucine α-carbons.

chemical shift as a tool for structural characterization as well as for the development of quantitative assessments of chain motion. Detailed information on the amplitudes and frequencies of motions in peptides and proteins is necessary for understanding the interaction between biopolymers. Direct measurements of atom-specific motional parameters (local correlation times and order parameters) require some model of the molecular structure and dynamics for complete interpretation. While homonuclear and heteronuclear chemical shift and coupling constant measurements generally do not give dynamical information on the nanosecond or shorter time scale, they may provide a useful starting model for dynamics calculations of an otherwise unknown system.

In these experiments the α-carbons exhibit a more consistent change in chemical shift than the α-protons over the range of the solvent titration and this uniform chemical shift variation can aid in the determination of helical secondary structure. Figure 4 demonstrates that while the disparate stabilities of the two halves of the molecule are also evident in both the proton and the carbon chemical shift changes, any arbitrarily chosen set of α-protons would not give a reliable indication of the aggregate amino acid configurations. In the range of concentrations from 100% to 60%, CD_3OD α-carbon resonances which show less migration, namely G1 through A4, L9, G12, and P14 through Q25, indicate small changes in shielding environment which could be accounted for by one of two structural processes; either the majority of that residue population is disposed in a non-helix configuration in high CD_3OD concentrations, or the helical configuration is more readily preserved for those residues as the methanol is diluted by water. The latter process is the

more likely for the non-terminal residues and suggests that there are local modulations in helix stability which are necessarily sequence specific.

As the methanol is diluted, G3 and G12 α-carbon resonances approach the average random coil chemical shift value typical of proteins in the Wishart (1991) database (44.0 ppm) but G1-C^{α} remains upfield. Figure 5 places some of the carbon chemical shifts of the terminal amino acids found in the HMQC series at 100% and 40% CD_3OD/D_2O in the context of the range of 90% of the values for each amino acid type found in protein secondary structures (from Fig. 4, Wishart et al., 1991). The α-carbon chemical shifts of all the residues migrate to lower values with a decrease in the organic fraction of the solvent (Fig. 4B), but the chemical shifts for some residues are outside the range of tabulated values appropriate for the supposed secondary structure. By comparison with the average chemical shift values for proteins, the first two residues of the amino-terminus are not involved in the helix at high methanol concentration although the I2 α-carbon signal does appear within the 90% chemical shift range of Wishart assignments. In contrast, α-carbon resonances of residues approaching the C-terminus appear downfield in the range of those observed in helical protein segments and migrate more slowly towards expected β-sheet values as the methanol/water ratio decreases. Comparisons of this type (see below) for the whole of the peptide sequence suggest that the helix-forming segment of the C-terminal half is more stable in the presence of water than is the amino-terminal half and that this is manifest in greater flexibility, or fraying, of the N-terminal residues in the helicogenic solvent. The C-terminal glutamine chemical shift changes are less than those of its nearest neighbors, indicating some chain fraying which involves fewer residues, and is less dramatic than that in the amino-terminus.

Our chemical shift data support the molecular dynamics simulation of the monomeric helix structure which led to the description of melittin behaving as two linked helices (Bazzo, 1988; Wesson and Eisenberg, 1992). G12 is situated near the middle of the sequence and in the simulations was shown to be the site of intrahelical instability owing to a defect in the hydrogen bond network due to P14. By comparing changes in chemical shift as a function of position relative to the peptide ends, one can demonstrate the different behaviors of the two helices. Considering the K7/K21 pair, residues of the same type and of approximately the same distance from the amino and carboxy termini respectively, the K7 $^{13}C^{\alpha}$ signal migrates 2.14 ppm between 100% and 40% methanol but the K21 resonance migrates only 1.10 ppm over this same solvent change. The K21 α-carbon resonance is 59.60 ppm in 100% CH_3OH and 58.85 ppm in 60%, but the K7 signal is 58.93 ppm and shifts to 57.67 ppm under these same conditions, indicating that not only is the amino terminus less stable as a helix in mixed solvents but it is also incompletely helical in neat methanol. Similar comparisons can be made for A4 and A15, as well as for L6 and L16, but their positions in the sequence must be considered individually. Some of the α-carbons in the C-terminal half which exhibit dramatic overall changes, P14, S18, K21, and Q25, are nearest neighbors along the hydrophilic face and this series is roughly in line with the i,i + 4 pattern observed for amide protons in protein helices (Zhou et al., 1992), which is evidence for an uncoiling mechanism beginning with helix bending followed by opening on the convex surface.

Wesson and Eisenberg (1992) have made a CHARMm dynamics simulation of a single melittin monomer extracted from the crystal structure with added atomic solvation parameters to improve the modeling of unfolding in water. In their study, the starting structure is helical but kinked at G12 and is similar to the NMR-derived structure proposed by Bazzo et al. In the Wesson and Eisenberg simulation, the C-terminal half is less stable than the first 11 residues with

solvation parameters omitted. However, the behavior of the peptide when solvation parameters are included is in greater agreement with results presented here; after 110 ps of CHARMm simulation the hydrophobic N-terminal half appears less helical in water than residues 16–22 with a slight unwinding of the four C-terminal residues. This pattern of helix unfolding in water is echoed in Figs. 4 and 5 where the chemical shifts of the α-carbons of residues 13–25 are less sensitive than those of residues 5–12 to increased proportions of water in the solvent mixture.

When a five-point running average of the chemical shifts along the amino acid sequence, suggested for proteins by Pastore and Saudek (1990), was applied to the proton and carbon data in Fig. 4 both the dramatic changes near G12 and the sawtooth patterns were obscured. Smoothed graphs of the secondary shift (calculated as the difference from random coil values) are also less informative. While valid for larger structures where tertiary structural interactions affect shielding environments, data smoothing may oversimplify structural interpretation when applied to short sequences.

Reily et al. (1992) have demonstrated an agreement between changes in ^{13}C chemical shift and the magnitude of the $[\theta]_{220}$ signal of the CD spectrum for the 14-amino acid bombesin sequence. Their comparison of the V^{10} C^{α} $\Delta\delta$ with the ellipticity at 220 nm provided evidence for a cooperative two-state transition induced by TFE with an inflection point near 20% TFE. The changes in chemical shifts for the melittin α-carbons do not suggest a single inflection point; each position in the sequence exhibits a smooth, but not necessarily sigmoidal, chemical shift dependence across the methanol titration range examined. Figure 4B does suggest that there is regional cooperativity in the uncoiling of the helix which is most evident in the range of residues from A15 to R24.

The reference chemical shifts of α-carbons in helical and extended residues are not yet well known: it is therefore not possible to reduce the chemical shift data of melittin in 100% methanol to a single percentage of helicity. Since a single resonance is observed for each backbone carbon, the CD results can now be interpreted in terms of a single population of partially folded peptides rather than as a set of folded and unfolded populations. A similar conclusion was reached by Liff et al. (1991) in a study of a set of designed peptides which compared CD spectra with several NMR observables: α-proton chemical shifts, NOEs between nearest neighbor NH protons, NOEs between NH and $C^{\alpha}H$ three residues along the chain, and $^{3}J_{H}{}^{\alpha}{}_{H}{}^{N}$ coupling constants.

Based on the measured $[\theta]_{222}$ in 100% methanol and a theoretical maximum of −40 deg cm^2 dmol^{-1} from Merutka et al. (1991), the CD results indicate that a maximum of 17 residues are involved in the melittin helix at 20 °C. On the other hand, the method of Greenfield and Fasman predicts that more than 90% of the 26 amino acids, or all but two residues, are involved in the helix at 100% methanol. The first approximation method by Greenfield–Fasman ignores the dependence of the CD signal strength on chain length and can thus overestimate the percent helicity of the hexacosa melittin but the scale proposed by Merutka et al. (1991) appears to underestimate the percent helicity. While single wavelength calculations are limited in their use of the information content of the CD spectrum (Johnson, 1990), they are an effective measure of the change in α-helix content for such a system (Yunes, 1982; Gans et al., 1991; Wilcox and Eisenberg, 1992). Standardization of the maximum helicity for short peptide chains remains unresolved; however, analysis of the $^{13}C^{\alpha}$ chemical shifts of melittin in the tetrameric form might provide sufficient data to correlate a limiting ellipticity for melittin with maximal helicity.

The separation of the α-proton resonances of G1, G3, and G12 generally is smaller with decreasing methanol concentration. As noted above, the splitting of the G1 α-proton lines ulti-

mately vanishes at both 40% and 15% methanol, while that of the G3 lines vanishes only at 15% methanol. This merger of the individual α-proton lines of G1 and G3 is most likely a result of chemical exchange due to an increased mobility of these residues in the random coil peptide. While the individual G1, G3, and G12 α-proton lines move closer to each other in the proton dimension as the methanol concentration is reduced below 100%, at methanol concentrations greater than 40% the lines do not show an appreciable broadening such as would occur if exchange were dominating in those circumstances. Apparently at intermediate methanol concentrations, the smaller line separations are primarily due to a direct solvent effect in which the chemical environments of the α-protons simply become less dissimilar. It is however unlikely that direct solvent effects alone could reduce the separation of the lines to zero since the G12 α-proton resonances are resolved even at 15% CD_3OD and at 100% D_2O as well (Brown et al., 1990). Furthermore at 15% CD_3OD, the G3 α-proton resonance is about 70% broader than that for G1 indicating that exchange is indeed operative for these residues at the lower methanol concentrations.

To determine the approximate magnitude of the exchange rate, we simulated the spectra including the scalar interaction of the α-protons with $J \sim 20$ Hz following the formalism of Kaplan and Fraenkel (1980). From the spectra at intermediate methanol concentrations, we estimate that the G1 and G3 α-proton singlets are averages of individual resonances that would be separated by 30 to 40 Hz in the absence of exchange. With a 40-Hz separation, the spectral simulations show that the exchange rate for G3 is on the order of 600 s^{-1} while that for G1 is greater than 4000 s^{-1}. Similarly with a 30-Hz separation, the simulations give an exchange rate for G3 on the order of 350 s^{-1} while that for G1 is greater than 3000 s^{-1}. These estimates apply to methanol concentrations of 40% and 15% for the G1 resonance and to 15% for the G3 resonance. Specific rates aside, it is clear that these data give further evidence of increased mobility in the N-terminal region of the peptide as it uncoils, with G1 showing the most mobility. In addition, these results are consistent with NMR relaxation measurements on melittin which are sensitive to motions on a much shorter time scale and which show the N-terminal glycines to have more motional freedom than other backbone residues (Buckley et al., 1993).

In this work we have reported the α-carbon chemical shifts of the 26-amino acid peptide melittin in methanol and methanol/water mixtures as determined from heteronuclear multiple quantum NMR spectra and previously published α-proton assignments. Changes in chemical shift are interpreted in terms of alterations in secondary structure with variations in solvent composition. We observe that the carbon frequency shifts of this short sequence are more easily interpreted than those of protons and that the changes vary more smoothly between residues. In light of the previous studies on proteins, and supporting studies on melittin, this work proposes that relative changes in the chemical shift during a titration of secondary structure are effective indicators of structural features, such as dynamical end fraying, for short peptide sequences and that absolute values will become more useful as the reference database of carbon chemical shifts is expanded.

ACKNOWLEDGEMENTS

This study was supported by NIH grant GM34847, NSF grant DMB-9105885, and by grants to the NMRFAM, which is supported in part by NIH grant RR02301 from the Biomedical

Research Technology Program, Division of Research Resources. Equipment in the NMRFAM was purchased with funds from the Biomedical Research Technology Program, the University of Wisconsin, the NSF Biological Instrumentation Program (grant DMB-8415048), the NIH Shared Instrument Program (grant RR02781), and the U.S. Department of Agriculture.

We gratefully acknowledge the assistance of Drs. William M. Westler, Stewart Loh, and Jasna Fejzo and Professor John L. Markley of the NMRFAM. We thank Dr. Sergei Venyaminov for technical assistance with the CD measurements and Phyllis Fisher and Peter Callahan for helpful discussions and technical support. We are indebted to Drs. Steve Landy and Jerry Kaplan, of IUPUI, for discussions of NMR spectral simulations and to Dr. Peng Yuan and Mr. Barry Waits, also of IUPUI, for their assistance in determining the effects of solvent composition on methanol chemical shifts.

REFERENCES

Bazzo, R., Tappin, M.J., Pastore, A., Harvey, T.S., Carver, J.A. and Campbell, I.D. (1988) *Eur. J. Biochem.*, **173**, 139–146.
Bello, J., Bello, H.R. and Granados, E. (1982) *Biochemistry*, **21**, 461–465.
Bax, A., Griffey, R.H. and Hawkins, B.L. (1983) *J. Magn. Reson.*, **55**, 301–315.
Braunschweiler, L. and Ernst, R.R. (1983) *J. Magn. Reson.*, **53**, 521–528.
Brown, L.R., Lauterwein, J. and Wüthrich, K. (1980) *Biochem. Biophys. Acta.*, **62**, 231–244.
Buckley, P.J., Kemple, M.D. and Prendergast, F.G. (1993) *J. Cell. Biochem.*, **17C**, 291.
Dempsey, C.E. (1988) *Biochemistry*, **27**, 6893–6901.
Kaplan, J.I. and Fraenkel, G. (1980) *NMR of Chemically Exchanging Systems*, Academic Press, New York.
Gans, P.J., Lyu, P.C., Manning, M.C., Woody, R.W. and Kallenbach, N.R. (1991) *Biopolymers*, **31**, 1605–1614.
Greenfield, N. and Fasman, G.D. (1969) *Biochemistry*, **8**, 4108–4116.
Habermann, E. (1972) *Science*, **177**, 314–322.
Ikura, T., Gō, N. and Inagaki, F. (1991) *Proteins: Struct. Func. Genet.*, **9**, 81–89.
Johnson, Jr., W.C. (1990) *Proteins: Struct. Func. Genet.*, **7**, 205–214.
Lakowicz, J.R., Gryczynski, I., Wiczk, W., Laczko, G., Prendergast, F.G. and Johnson, M. (1990) *Biophys. Chem.*, **36**, 99–115.
Lauterwein, J., Brown, L.R. and Wüthrich, K. (1980) *Biochem. Biophys. Acta.*, **622**, 219–230.
Liff, M.I., Lyu, P.C. and Kallenbach, N.R. (1991) *J. Am. Chem. Soc.*, **113**, 1014–1019.
Merutka, G., Shalongo, W. and Stellwagen, E. (1991) *Biochemistry*, **30**, 4245–4248.
Müller, L. (1979) *J. Am. Chem. Soc.*, **101**, 4481–4484.
Pastore, A., Harvey, T.S., Dempsey, C.E. and Campbell, I.D. (1989) *Eur. Biophys. J.*, **16**, 363–367.
Pastore, A. and Saudek, V. (1990) *J. Magn. Reson.*, **90**, 165–176.
Quay, S.C. and Condie, C.C. (1983) *Biochemistry*, **22**, 695–700.
Reily, M.D., Venkataraman, T. and Omecinsky, D.O. (1992) *J. Am. Chem. Soc.*, **114**, 6251–6252.
Schwarz, G. *J. Mol. Biol.* (1965), **11**, 64–77.
Spera, S. and Bax, A. *J. Am. Chem. Soc.* (1991), **113**, 5490–5492.
Terwillinger, T.C. and Eisenberg, D. (1982a) *J. Biol. Chem.*, **257**, 6010–6015.
Terwillinger, T.C. and Eisenberg, D. (1982b) *J. Biol. Chem.*, **257**, 6016–6022.
Wesson, L. and Eisenberg, D. (1992) *Protein Sci.*, **1**, 227–235.
Weaver, A.J., Kemple, M.D., Brauner, J.W., Mendelson, R. and Prendergast, F.G. (1992) *Biochemistry*, **28**, 1301–1313.
Weaver, A.J., Kemple, M.D. and Prendergast, F.G. (1989) *Biochemistry*, **28**, 8614–8623.
Wilcox, W. and Eisenberg, D. (1992) *Protein Sci.*, **1**, 641–653.
Wishart, D.S., Sykes, B.D. and Richards, F.M. (1991) *J. Mol. Biol.*, **222**, 311–333.
Yunes, R.A. (1982) *Arch. Biochem. Biophys.*, **216**, 559–565.
Zhou, N.E., Zhu, B., Sykes, B.D. and Hodges, R.S. (1992) *J. Am. Chem. Soc.*, **114**, 4320–4326.